BELLE-CONF-0401
ICHEP 11-0646

Search for the $b \to d\gamma$ process

K. Abe,[10] K. Abe,[46] N. Abe,[49] I. Adachi,[10] H. Aihara,[48] M. Akatsu,[24] Y. Asano,[53] T. Aso,[52] V. Aulchenko,[2] T. Aushev,[14] T. Aziz,[44] S. Bahinipati,[6] A. M. Bakich,[43] Y. Ban,[36] M. Barbero,[9] A. Bay,[20] I. Bedny,[2] U. Bitenc,[15] I. Bizjak,[15] S. Blyth,[29] A. Bondar,[2] A. Bozek,[30] M. Bračko,[22,15] J. Brodzicka,[30] T. E. Browder,[9] M.-C. Chang,[29] P. Chang,[29] Y. Chao,[29] A. Chen,[26] K.-F. Chen,[29] W. T. Chen,[26] B. G. Cheon,[4] R. Chistov,[14] S.-K. Choi,[8] Y. Choi,[42] Y. K. Choi,[42] A. Chuvikov,[37] S. Cole,[43] M. Danilov,[14] M. Dash,[55] L. Y. Dong,[12] R. Dowd,[23] J. Dragic,[23] A. Drutskoy,[6] S. Eidelman,[2] Y. Enari,[24] D. Epifanov,[2] C. W. Everton,[23] F. Fang,[9] S. Fratina,[15] H. Fujii,[10] N. Gabyshev,[2] A. Garmash,[37] T. Gershon,[10] A. Go,[26] G. Gokhroo,[44] B. Golob,[21,15] M. Grosse Perdekamp,[38] H. Guler,[9] J. Haba,[10] F. Handa,[47] K. Hara,[10] T. Hara,[34] N. C. Hastings,[10] K. Hasuko,[38] K. Hayasaka,[24] H. Hayashii,[25] M. Hazumi,[10] E. M. Heenan,[23] I. Higuchi,[47] T. Higuchi,[10] L. Hinz,[20] T. Hojo,[34] T. Hokuue,[24] Y. Hoshi,[46] K. Hoshina,[51] S. Hou,[26] W.-S. Hou,[29] Y. B. Hsiung,[29] H.-C. Huang,[29] T. Igaki,[24] Y. Igarashi,[10] T. Iijima,[24] A. Imoto,[25] K. Inami,[24] A. Ishikawa,[10] H. Ishino,[49] K. Itoh,[48] R. Itoh,[10] M. Iwamoto,[3] M. Iwasaki,[48] Y. Iwasaki,[10] R. Kagan,[14] H. Kakuno,[48] J. H. Kang,[56] J. S. Kang,[17] P. Kapusta,[30] S. U. Kataoka,[25] N. Katayama,[10] H. Kawai,[3] H. Kawai,[48] Y. Kawakami,[24] N. Kawamura,[1] T. Kawasaki,[32] N. Kent,[9] H. R. Khan,[49] A. Kibayashi,[49] H. Kichimi,[10] H. J. Kim,[19] H. O. Kim,[42] Hyunwoo Kim,[17] J. H. Kim,[42] S. K. Kim,[41] T. H. Kim,[56] K. Kinoshita,[6] P. Koppenburg,[10] S. Korpar,[22,15] P. Križan,[21,15] P. Krokovny,[2] R. Kulasiri,[6] C. C. Kuo,[26] H. Kurashiro,[49] E. Kurihara,[3] A. Kusaka,[48] A. Kuzmin,[2] Y.-J. Kwon,[56] J. S. Lange,[7] G. Leder,[13] S. E. Lee,[41] S. H. Lee,[41] Y.-J. Lee,[29] T. Lesiak,[30] J. Li,[40] A. Limosani,[23] S.-W. Lin,[29] D. Liventsev,[14] J. MacNaughton,[13] G. Majumder,[44] F. Mandl,[13] D. Marlow,[37] T. Matsuishi,[24] H. Matsumoto,[32] S. Matsumoto,[5] T. Matsumoto,[50] A. Matyja,[30] Y. Mikami,[47] W. Mitaroff,[13] K. Miyabayashi,[25] Y. Miyabayashi,[24] H. Miyake,[34] H. Miyata,[32] R. Mizuk,[14] D. Mohapatra,[55] G. R. Moloney,[23] G. F. Moorhead,[23] T. Mori,[49] A. Murakami,[39] T. Nagamine,[47] Y. Nagasaka,[11] T. Nakadaira,[48] I. Nakamura,[10] E. Nakano,[33] M. Nakao,[10] H. Nakazawa,[10] Z. Natkaniec,[30] K. Neichi,[46] S. Nishida,[10] O. Nitoh,[51] S. Noguchi,[25] T. Nozaki,[10] A. Ogawa,[38] S. Ogawa,[45] T. Ohshima,[24] T. Okabe,[24] S. Okuno,[16] S. L. Olsen,[9] Y. Onuki,[32] W. Ostrowicz,[30] H. Ozaki,[10] P. Pakhlov,[14] H. Palka,[30] C. W. Park,[42] H. Park,[19] K. S. Park,[42] N. Parslow,[43] L. S. Peak,[43] M. Pernicka,[13] J.-P. Perroud,[20] M. Peters,[9] L. E. Piilonen,[55] A. Poluektov,[2] F. J. Ronga,[10] N. Root,[2] M. Rozanska,[30] H. Sagawa,[10] M. Saigo,[47] S. Saitoh,[10] Y. Sakai,[10] H. Sakamoto,[18] T. R. Sarangi,[10] M. Satapathy,[54] N. Sato,[24] O. Schneider,[20] J. Schümann,[29] C. Schwanda,[13] A. J. Schwartz,[6] T. Seki,[50] S. Semenov,[14] K. Senyo,[24] Y. Settai,[5] R. Seuster,[9] M. E. Sevior,[23] T. Shibata,[32] H. Shibuya,[45] B. Shwartz,[2] V. Sidorov,[2] V. Siegle,[38] J. B. Singh,[35] A. Somov,[6] N. Soni,[35] R. Stamen,[10] S. Stanič,[53,*] M. Starič,[15] A. Sugi,[24] A. Sugiyama,[39] K. Sumisawa,[34] T. Sumiyoshi,[50] S. Suzuki,[39] S. Y. Suzuki,[10] O. Tajima,[10] F. Takasaki,[10] K. Tamai,[10] N. Tamura,[32] K. Tanabe,[48] M. Tanaka,[10] G. N. Taylor,[23] Y. Teramoto,[33] X. C. Tian,[36] S. Tokuda,[24] S. N. Tovey,[23] K. Trabelsi,[9] T. Tsuboyama,[10]

T. Tsukamoto,[10] K. Uchida,[9] S. Uehara,[10] T. Uglov,[14] K. Ueno,[29] Y. Unno,[3] S. Uno,[10] Y. Ushiroda,[10] G. Varner,[9] K. E. Varvell,[43] S. Villa,[20] C. C. Wang,[29] C. H. Wang,[28] J. G. Wang,[55] M.-Z. Wang,[29] M. Watanabe,[32] Y. Watanabe,[49] L. Widhalm,[13] Q. L. Xie,[12] B. D. Yabsley,[55] A. Yamaguchi,[47] H. Yamamoto,[47] S. Yamamoto,[50] T. Yamanaka,[34] Y. Yamashita,[31] M. Yamauchi,[10] Heyoung Yang,[41] P. Yeh,[29] J. Ying,[36] K. Yoshida,[24] Y. Yuan,[12] Y. Yusa,[47] H. Yuta,[1] S. L. Zang,[12] C. C. Zhang,[12] J. Zhang,[10] L. M. Zhang,[40] Z. P. Zhang,[40] V. Zhilich,[2] T. Ziegler,[37] D. Žontar,[21,15] and D. Zürcher[20]

(The Belle Collaboration)

[1]*Aomori University, Aomori*
[2]*Budker Institute of Nuclear Physics, Novosibirsk*
[3]*Chiba University, Chiba*
[4]*Chonnam National University, Kwangju*
[5]*Chuo University, Tokyo*
[6]*University of Cincinnati, Cincinnati, Ohio 45221*
[7]*University of Frankfurt, Frankfurt*
[8]*Gyeongsang National University, Chinju*
[9]*University of Hawaii, Honolulu, Hawaii 96822*
[10]*High Energy Accelerator Research Organization (KEK), Tsukuba*
[11]*Hiroshima Institute of Technology, Hiroshima*
[12]*Institute of High Energy Physics, Chinese Academy of Sciences, Beijing*
[13]*Institute of High Energy Physics, Vienna*
[14]*Institute for Theoretical and Experimental Physics, Moscow*
[15]*J. Stefan Institute, Ljubljana*
[16]*Kanagawa University, Yokohama*
[17]*Korea University, Seoul*
[18]*Kyoto University, Kyoto*
[19]*Kyungpook National University, Taegu*
[20]*Swiss Federal Institute of Technology of Lausanne, EPFL, Lausanne*
[21]*University of Ljubljana, Ljubljana*
[22]*University of Maribor, Maribor*
[23]*University of Melbourne, Victoria*
[24]*Nagoya University, Nagoya*
[25]*Nara Women's University, Nara*
[26]*National Central University, Chung-li*
[27]*National Kaohsiung Normal University, Kaohsiung*
[28]*National United University, Miao Li*
[29]*Department of Physics, National Taiwan University, Taipei*
[30]*H. Niewodniczanski Institute of Nuclear Physics, Krakow*
[31]*Nihon Dental College, Niigata*
[32]*Niigata University, Niigata*
[33]*Osaka City University, Osaka*
[34]*Osaka University, Osaka*
[35]*Panjab University, Chandigarh*
[36]*Peking University, Beijing*
[37]*Princeton University, Princeton, New Jersey 08545*

[38]RIKEN BNL Research Center, Upton, New York 11973
[39]Saga University, Saga
[40]University of Science and Technology of China, Hefei
[41]Seoul National University, Seoul
[42]Sungkyunkwan University, Suwon
[43]University of Sydney, Sydney NSW
[44]Tata Institute of Fundamental Research, Bombay
[45]Toho University, Funabashi
[46]Tohoku Gakuin University, Tagajo
[47]Tohoku University, Sendai
[48]Department of Physics, University of Tokyo, Tokyo
[49]Tokyo Institute of Technology, Tokyo
[50]Tokyo Metropolitan University, Tokyo
[51]Tokyo University of Agriculture and Technology, Tokyo
[52]Toyama National College of Maritime Technology, Toyama
[53]University of Tsukuba, Tsukuba
[54]Utkal University, Bhubaneswer
[55]Virginia Polytechnic Institute and State University, Blacksburg, Virginia 24061
[56]Yonsei University, Seoul

(Dated: August 18 2004)

Abstract

We report search results for the flavor-changing neutral current process $b \to d\gamma$ with a data sample containing 274 million B meson pairs accumulated at the $\Upsilon(4S)$ resonance with the Belle detector at KEKB. We studied the exclusive decays $B^- \to \rho^-\gamma$, $\overline{B}^0 \to \rho^0\gamma$, and $\overline{B}^0 \to \omega\gamma$, and find no significant signal. We set an upper limit for a combined branching fraction $\mathcal{B}(B \to (\rho,\omega)\gamma) < 1.4 \times 10^{-6}$ at the 90% confidence level, which is normalized to that of $B^- \to \rho^-\gamma$ assuming an isospin relation between the three modes.

PACS numbers: 11.30.Hv, 13.40.Hq, 14.65.Fy, 14.40.Nd

The $b \to d\gamma$ process, shown in Fig. 1(a), is a flavor changing neutral current transition that proceeds via loop diagrams in the Standard Model (SM). It is suppressed with respect to $b \to s\gamma$ by the Cabibbo-Kobayashi-Maskawa (CKM) factor $|V_{td}/V_{ts}|^2 \sim 0.04$ with a large uncertainty due to the lack of precise knowledge of V_{td}. The exclusive modes $B \to \rho\gamma$ and $\omega\gamma$, which are presumably dominant, have not yet been observed [1, 2]. They are also suppressed with respect to the corresponding exclusive decay $B \to K^*\gamma$ by $|V_{td}/V_{ts}|^2$, with corrections due to form factors, $SU(3)$ breaking effects and the additional annihilation diagrams (Fig. 1(b)), giving predicted branching fractions in the range $(0.9\text{–}2.7) \times 10^{-6}$ in the SM [3, 4]. Measurement of these exclusive branching fractions would improve the constraints on V_{td} in the context of the SM, and would provide sensitivity to physics beyond the SM that is complementary to that from $b \to s\gamma$.

In this paper, we report the results of a search for the $b \to d\gamma$ process using a data sample of (274 ± 3) million B meson pairs accumulated at the $\Upsilon(4S)$ resonance. The data are produced in e^+e^- annihilation at the KEKB energy-asymmetric (3.5 on 8 GeV) collider [5] and collected with the Belle detector [6]. The Belle detector is a large-solid-angle spectrometer that includes a silicon vertex detector (SVD), a central drift chamber (CDC), an array of aerogel threshold Cherenkov counters (ACC), time-of-flight (TOF) scintillation counters, and an electromagnetic calorimeter (ECL) comprised of CsI(Tl) crystals located inside a superconducting solenoid coil that provides a 1.5 T magnetic field. An iron flux-return located outside of the coil is instrumented to identify muons (KLM). The dataset consists of two subsets with different inner detector configurations: for the first 152 million B meson pairs, a 2.0 cm radius beampipe and a 3-layer SVD were used; and for the remaining 122 million B meson pairs, a 1.5 cm radius beampipe, a 4-layer SVD and a small-cell inner drift chamber were used [7].

We reconstruct the following final states: $B^- \to \rho^-\gamma$, $\overline{B}^0 \to \rho^0\gamma$, and $\overline{B}^0 \to \omega\gamma$. (Charge conjugate modes are implied throughout this paper.) We also reconstruct control samples of $B^- \to K^{*-}\gamma$ and $\overline{B}^0 \to \overline{K}^{*0}\gamma$ decays. The following decay chains are used to reconstruct the intermediate states: $\rho^- \to \pi^-\pi^0$, $\rho^0 \to \pi^+\pi^-$, $\omega \to \pi^+\pi^-\pi^0$, $K^{*-} \to K^-\pi^0$, $\overline{K}^{*0} \to K^-\pi^+$, and $\pi^0 \to \gamma\gamma$.

Photon candidates are reconstructed from isolated clusters in the ECL that have no corresponding charged track, and a shower shape that is consistent with that of a photon. The photon with the largest center-of-mass (CM) energy in the range 1.4 GeV $< E_\gamma <$ 3.4 GeV and in the barrel region of the ECL ($33^\circ < \theta_\gamma < 128^\circ$ in the laboratory frame) is selected as the primary photon candidate. To suppress backgrounds from $\pi^0 \to \gamma\gamma$ and $\eta \to \gamma\gamma$ decays, we veto the event if the reconstructed mass of the primary photon and any other photon of 30 (200) MeV or more is within ± 18 (32) MeV/c^2 of the π^0 (η) mass. These correspond to $\pm 3\sigma$ windows, where σ is the mass resolution. This set of criteria is referred to as the π^0/η veto. For the primary photon, we sum the energy deposited in arrays of 3×3 cells and 5×5 cells around the maximum energy ECL cell; if their ratio is less than 0.95, the event is vetoed.

Charged pions and kaons are reconstructed as tracks in the CDC and SVD. Each track is required to have a momentum greater than 100 MeV/c and closest approach to the run-averaged interaction point within 2 cm in radius and ± 5 cm along the z-axis, aligned opposite the positron beam. We do not use the track to form the signal candidate if, when combined with any other track, it forms a K^0_S candidate with a mass within ± 10 MeV/c^2 around the nominal K^0_S mass and a displaced vertex that is consistent with a K^0_S. We determine the pion (L_π) and kaon (L_K) likelihoods from the ACC response, specific ionization

(dE/dx) in the CDC and TOF flight-time measurements for each track, and form a likelihood ratio $\mathcal{L}_{\pi/K} = L_\pi/(L_\pi + L_K)$ to separate pions and kaons. We require $\mathcal{L}_{\pi/K} > 0.85$ for pions, which gives an efficiency of 89% for pions and misidentification probability of $\sim$10% for kaons. For the $\omega\gamma$ mode, we relax the requirement to $\mathcal{L}_{\pi/K} > 0.8$, which gives an efficiency of 94% for pions. (For kaons in the $K^*\gamma$ modes, we require $\mathcal{L}_{\pi/K} < 0.4$, which gives an efficiency of 76–80%.) In addition, we remove pion and kaon candidates if they are consistent with being electrons based on ECL, dE/dx and ACC information, or consistent with muons based on KLM information.

Neutral pions are formed from two photons with invariant masses within ± 10 (16) MeV/c^2 of the π^0 mass, corresponding to a $\sim 2\sigma$ ($\sim 3\sigma$) window for $\rho^-\gamma$ and $K^{*-}\gamma$ ($\omega\gamma$) modes. The photon momenta are then recalculated with a π^0 mass constraint. We require each photon energy to be greater than 30 MeV. We also require the CM momentum of the π^0 to be greater than 0.5 GeV/c for the $\rho^-\gamma$ and $K^{*-}\gamma$ modes.

Invariant masses for the ρ and ω candidates are required to be within windows of ± 150 MeV/c^2 (1Γ) and ± 30 MeV/c^2 (3.5Γ), respectively, around their nominal masses, where Γ is the natural width of each resonance.

We form B candidates by combining a ρ or ω candidate and the primary photon using two variables: the beam-energy constrained mass $M_{\rm bc} = \sqrt{(E^*_{\rm beam}/c^2)^2 - |p^*_B/c|^2}$ and the energy difference $\Delta E = E^*_B - E^*_{\rm beam}$, where p^*_B and E^*_B are the measured CM momentum and energy, respectively, of the B candidate, and $E^*_{\rm beam}$ is the CM beam energy. The magnitude of the photon momentum is replaced by $(E^*_{\rm beam} - E^*_{\rho/\omega})/c$ when the momentum p^*_B is calculated. To optimize the event selection, we count Monte Carlo (MC) events in the region -0.10 GeV $< \Delta E < 0.08$ GeV and 5.273 GeV/$c^2 < M_{\rm bc} < 5.285$ GeV/c^2. We choose the selection criteria to maximize $N_S/\sqrt{N_B}$, where N_S is the expected signal yield in this region assuming the branching fractions to be the SM value in Ref. [3], and N_B is the expected background yield in the same region.

The dominant background arises from continuum events ($e^+e^- \to q\overline{q}(\gamma)$) where the accidental combination of a ρ or ω candidate with a photon forms a B candidate. We suppress this background using an event shape discriminator $\mathcal{F}$, the B candidate polar angle θ^*_B in the CM frame, the vertex separation Δz, and the output of the B-flavor tagging algorithm:

1. The event shape discriminator $\mathcal{F}$ [8] is a Fisher discriminant [9] constructed from 16 modified Fox-Wolfram moments [8, 10] and the scalar sum of the transverse momentum of all charged tracks and photons.

2. True B mesons follow a $1 - \cos^2\theta^*_B$ distribution in $\cos\theta^*_B$, while candidates in the continuum background are uniformly distributed.

3. In about 85% of events for the $\rho^0\gamma$ and $\omega\gamma$ modes, a fit can be successfully performed to determine the decay vertex of the candidate B meson as well as the origin of the remaining tracks in the event. The separation Δz between these two vertices along the z-axis discriminates between continuum events, which have a common vertex, and signal events, whose decay vertices are displaced.

4. The B-flavor tagging algorithm described in Ref. [11] returns the flavor of the other B meson ($q = \pm 1$), and a tagging quality r ($0 < r < 1$) which indicates the level of confidence in the flavor determination. The algorithm uses the particles in the event that are not associated with the signal B candidate, and provides additional

discrimination between signal, and continuum background where no true B meson is present.

For each of the quantities $\mathcal{F}$, $\cos\theta_B^*$ and Δz, we construct one-dimensional likelihood distributions for signal and continuum. Signal distributions are modeled with an asymmetric Gaussian function for $\mathcal{F}$, $\frac{3}{2}(a_0 - a_2\cos^2\theta_B^*)$ for $\cos\theta_B^*$, and an exponential convolved with a Gaussian resolution function for Δz; continuum background distributions are modeled with an asymmetric Gaussian function for $\mathcal{F}$, $(b_0 - b_2\cos^2\theta_B^*)$ for $\cos\theta_B^*$, and a sum of three Gaussian functions with a common mean for Δz; the coefficients a_0, a_2, b_0 are close to unity while the coefficient b_2 is close to zero.

Since $\mathcal{F}$, $\cos\theta_B^*$ and Δz are independent quantities, we form a likelihood ratio $\mathcal{R} = \mathcal{L}_s/(\mathcal{L}_s + \mathcal{L}_c)$ to combine them, where $\mathcal{L}_s$ and $\mathcal{L}_c$ are products of $\mathcal{F}$, $\cos\theta_B^*$ (and Δz if available) likelihood distributions for signal and continuum, respectively. The likelihood distribution for the background Δz distribution is determined from data in the sideband region 5.20 GeV/$c^2 < M_{\rm bc} <$ 5.24 GeV/c^2, $|\Delta E| < 0.3$ GeV; all the other likelihood distributions are determined from MC samples.

We determine the Δz likelihood function separately for the two datasets as the vertex resolution is improved in the SVD2 with respect to the SVD1. As a consequence, we introduce two sets of likelihood ratios and selection criteria for each decay mode.

On the plane defined by the tagging quality and likelihood ratio, $(r, \mathcal{R})$, signal tends to populate the edges at $r = 1$ and $\mathcal{R} = 1$; continuum tends to populate the edges at $r = 0$ and $\mathcal{R} = 0$. We select the events in a signal enriched region defined by $\mathcal{R} > \mathcal{R}_1$ for $r > r_1$, and $\mathcal{R} > 1 - \alpha(1 + r)$ for $r_2 < r < r_1$, where the parameters r_1, r_2, R_1 and α are mode dependent and are determined so that $N_S/\sqrt{N_S + N_B}$ is maximized (we use this quantity instead of $N_S/\sqrt{N_B}$ because of the limited statistics of the MC simulation sample that is used in this procedure). The values are $r_1 = 0.85$, $r_2 = 0.01$, $R_1 > 0.8$ and $\alpha = 0.025$ for the $\rho^0\gamma$ mode in the first subset of data; similar values are used for the other subset and for the $\rho^-\gamma$ and $\omega\gamma$ modes. We define the rest of the area as the background enriched region.

We consider the following B decay backgrounds: $B \to K^*\gamma$, other $B \to X_s\gamma$ processes, $B \to \rho\pi^0$ and $\omega\pi^0$, $B \to \rho\eta$ and $\omega\eta$, $B^- \to \rho^-\rho^0$, other charmless B decays, and $b \to c$ backgrounds. We find the $b \to c$ background to be negligible. The $B \to K^*\gamma$ background may mimic the signal decay $B \to \rho\gamma$ if the kaon from K^* is misidentified as a pion. In order to further suppress $B \to K^*\gamma$, we calculate $M_{K\pi}$, where the kaon mass is assigned to one of the pion candidates, and reject the candidate if $M_{K\pi} < 0.96$ (0.92) GeV/c^2 for the $\rho^0\gamma$ ($\rho^-\gamma$) mode. The decay chain $\overline{B}^0 \to \overline{K}^{*0}\gamma$, $\overline{K}^{*0} \to K^0_S\pi^0$, $K^0_S \to \pi^+\pi^-$ has the same final state as $\overline{B}^0 \to \omega\gamma$, and has a small contribution due to the tail of the K^* Breit-Wigner line shape. In addition, $B \to K^*\gamma$ and other $B \to X_s\gamma$ decays contribute to the background when the ρ and ω candidates are selected from a random combination of particles. Charmless decays with a π^0 or $\eta \to \gamma\gamma$, $B \to \rho\pi^0$, $\omega\pi^0$, $\rho\eta$ and $\omega\eta$, may mimic the signal if one of the photons from π^0 or η decay is soft and undetected by the π^0/η veto condition. To suppress this background, we calculate the cosine of the helicity angle $\theta_{\rm hel}$, and reject the candidate if $|\cos\theta_{\rm hel}| > 0.8$ (0.6) for the $\rho^0\gamma$ and $\omega\gamma$ ($\rho^-\gamma$) modes. Here, $\theta_{\rm hel}$ is defined as the angle between the π^+ and B momentum vectors in the ρ rest frame, or the angle between the normal to the ω decay plane and the B momentum vector in the ω rest frame. The decay $B^- \to \rho^-\rho^0$, $\rho^- \to \pi^-\pi^0$ also contributes to the $B^0 \to \rho^0\gamma$ mode when both one pion from the ρ^- decay and one photon from the π^0 decay are soft and undetected. The other charmless decays have small contributions and are considered as an additional background component when we extract the signal yield.

The reconstruction efficiency for each mode is defined by the fraction of the signal yield remaining after all selection criteria, where the signal yield is determined from an extended unbinned maximum likelihood fit to the MC sample. The signal distributions are modeled as the product of a Gaussian function for $M_{\rm bc}$ and an empirical function known as the Crystal Ball line shape [12] to reproduce the asymmetric ECL energy response for ΔE. The background component is modeled as the product of a linear function for ΔE, and an ARGUS function [13] for $M_{\rm bc}$. From the fit, we find efficiencies of about 5% as listed in Table I. The systematic error on the efficiency is the quadratic sum of the following contributions estimated from control samples: the photon detection efficiency (2.2%), measured from radiative Bhabha events; charged tracking efficiency (1.0% per track) from partially reconstructed $D^{*+} \to D^0\pi^+$, $D^0 \to K^0_S\pi^+\pi^-$, $K^0_S \to \pi^+(\pi^-)$; charged pion identification (1.0% per pion) from $D^{*+} \to D^0\pi^+$, $D^0 \to K^-\pi^+$; neutral pion detection (4.6–7.3%) from η decays to $\gamma\gamma$, $\pi^+\pi^-\pi^0$ and $3\pi^0$; $\mathcal{R}$-r and π^0/η veto requirements (5.4%) from $B^- \to D^0\pi^-$, $D^0 \to K^-\pi^+$; and MC statistics (0.9–1.5%).

We perform an unbinned maximum likelihood fit to the data in the ($M_{\rm bc}$, ΔE) fit region bounded by $|\Delta E| < 0.3$ GeV and $M_{\rm bc} > 5.2$ GeV/c^2, simultaneously for the three signal modes (collectively referred to as $B \to (\rho,\omega)\gamma$) and the two $B \to K^*\gamma$ modes. We fit the two data subsets simultaneously, so that in total ten distributions are included in the fit. We define the combined branching fraction $\mathcal{B}(B \to (\rho,\omega)\gamma) = \mathcal{B}(B^- \to \rho^-\gamma)$, assuming the isospin relation [14] $\mathcal{B}(B^- \to \rho^-\gamma) = 2\frac{\tau_{B^+}}{\tau_{B^0}}\mathcal{B}(\overline{B}^0 \to \rho^0\gamma) = 2\frac{\tau_{B^+}}{\tau_{B^0}}\mathcal{B}(\overline{B}^0 \to \omega\gamma)$, where we use $\frac{\tau_{B^+}}{\tau_{B^0}} = 1.086 \pm 0.017$ [16]. We also assume $\mathcal{B}(B \to K^*\gamma) \equiv \mathcal{B}(B^- \to K^{*-}\gamma) = \frac{\tau_{B^+}}{\tau_{B^0}}\mathcal{B}(\overline{B}^0 \to \overline{K}^{*0}\gamma)$.

We describe the events in the fit region using a sum of the signal, continuum, $K^*\gamma$, and other background hypotheses. Parameters of the signal description for $M_{\rm bc}$ are calibrated using $B^- \to D^0\pi^-$ samples. Those for ΔE are calibrated using the result of a fit to the ΔE distribution of the $B \to K^*\gamma$ control sample, in which the mean and the width are allowed to float. We use the branching fractions for $B \to (\rho,\omega)\gamma$ and $B \to K^*\gamma$ as the free parameters, from which the signal yield for each channel is deduced using the efficiency for each mode. We assume the efficiency systematic errors are fully correlated when we evaluate the systematic error. The continuum background is modeled as the product of a linear function for ΔE whose slope is allowed to float, and an ARGUS function for $M_{\rm bc}$ whose parameters are fixed from a comparison between data and MC in the background enriched region and MC in the signal enriched region. The continuum contribution in the data sample is allowed to float. The size of the $K^*\gamma$ background component in each $(\rho,\omega)\gamma$ channel is constrained using the fit to the $K^*\gamma$ events. The contributions of the other backgrounds are fixed using known branching fractions or upper limits. The free parameters in the fit are therefore the branching fractions for $B \to (\rho,\omega)\gamma$ and $B \to K^*\gamma$, five continuum fractions, and five continuum ΔE slopes.

We also perform individual fits to the three signal modes and the two $B \to K^*\gamma$ modes. The two data subsets are fitted simultaneously for each mode. The size of the $\overline{K}^{*0}\gamma$ background in the $\rho^0\gamma$ mode and $K^{*-}\gamma$ background in the $\rho^-\gamma$ mode are fixed according to the fit results to the $B \to K^*\gamma$ modes and the known particle misidentification probabilities. The free parameters in each fit are the signal yield, the continuum fraction, and the continuum ΔE slope.

Results of the simultaneous fit are shown in Fig. 2 and given in Table I. The simultaneous fit gives a significance of 1.9 standard deviations, where the significance is calculated as

$\sqrt{-2\ln(\mathcal{L}_0/\mathcal{L}_{\rm max})}$, and $\mathcal{L}_{\rm max}$ ($\mathcal{L}_0$) is the maximum likelihood from the fit when the signal branching fraction is floated (constrained to be zero). In order to include the effect of possible systematic error in the significance calculation, we change each parameter by one standard deviation in the direction that gives the smallest resulting significance. The systematic error in the signal yield is estimated by varying each of the fixed parameters by its standard deviation, and then taking the quadratic sum of the deviations in the signal yield from the nominal value. The combined branching fraction is $\mathcal{B}(B \to (\rho,\omega)\gamma) = (0.72\,^{+0.43\,+0.28}_{-0.39\,-0.27}) \times 10^{-6}$, where the first and second errors are statistical and systematic, respectively.

Since the significance is small, we quote a 90% confidence level upper limit $\mathcal{B}_{90}$ using the relation $\int_0^{\mathcal{B}_{90}} \mathcal{L}(x)dx = 0.9\int_0^{\infty} \mathcal{L}(x)dx$, where $\mathcal{L}(x)$ is the likelihood function with the branching fraction fixed at x. The systematic error is taken into account assuming a Gaussian distribution. We find

$$\mathcal{B}(B \to (\rho,\omega)\gamma) < 1.4 \times 10^{-6} \tag{1}$$

at the 90% confidence level. Results of the fits to the individual modes are also given in Table I.

A similar fit procedure is performed by using the ratio of branching fractions $\mathcal{B}(B \to (\rho,\omega)\gamma)/\mathcal{B}(B \to K^*\gamma)$ instead of $\mathcal{B}(B \to (\rho,\omega)\gamma)$, so that the systematic error partially cancels. We find $\mathcal{B}(B \to (\rho,\omega)\gamma)/\mathcal{B}(B \to K^*\gamma) < 0.035$ at the 90% confidence level. One can use this result to constrain V_{td}: for example, using the prescription given in Ref. [15],

$$\frac{\mathcal{B}(B \to (\rho,\omega)\gamma)}{\mathcal{B}(B \to K^*\gamma)} = \left|\frac{V_{td}}{V_{ts}}\right|^2 \frac{(1-m^2_{(\rho,\omega)}/m^2_B)^3}{(1-m^2_{K^*}/m^2_B)^3}\zeta^2[1+\Delta R] \tag{2}$$

where the form factor ratio $\zeta = 0.85 \pm 0.10$ and $SU(3)$ breaking effect $\Delta R = 0.1 \pm 0.1$, we obtain $|V_{td}/V_{ts}| < 0.21$ at the 90% confidence level. This limit is consistent with other determinations of $|V_{td}/V_{ts}|$ [16].

In conclusion, we search for the $b \to d\gamma$ process using a simultaneous fit to the $B \to \rho\gamma$, $\overline{B}^0 \to \omega\gamma$ and $B \to K^*\gamma$ modes. The upper limit we obtain is already within the range of SM predictions [3, 4] and can be used to constrain V_{td}.

We wish to thank the KEKB accelerator group for the excellent operation of the KEKB accelerator. We acknowledge support from the Ministry of Education, Culture, Sports, Science, and Technology of Japan and the Japan Society for the Promotion of Science; the Australian Research Council and the Australian Department of Education, Science and Training; the National Science Foundation of China under contract No. 10175071; the Department of Science and Technology of India; the BK21 program of the Ministry of Education of Korea and the CHEP SRC program of the Korea Science and Engineering Foundation; the Polish State Committee for Scientific Research under contract No. 2P03B 01324; the Ministry of Science and Technology of the Russian Federation; the Ministry of Education, Science and Sport of the Republic of Slovenia; the National Science Council and the Ministry of Education of Taiwan; and the U.S. Department of Energy.

---

* on leave from Nova Gorica Polytechnic, Nova Gorica

[1] M. Nakao (for the Belle Collaboration), hep-ex/0307031.

[2] BaBar Collaboration, B. Aubert *et al.*, Phys. Rev. Lett. **92**, 111801 (2004).

[3] A. Ali and A. Ya. Parkhomenko, Eur. Phys. J. C **23**, 89 (2002).

[4] In addition to Ref. [3], for example, S. Bosch and G. Buchalla, Nucl. Phys. B **621**, 459 (2002); T. Huang, Z. Li and H. Zhang, J. Phys. G **25**, 1179 (1999).
[5] S. Kurokawa and E. Kikutani, Nucl. Instrum. Meth. A **499**, 1 (2003).
[6] Belle Collaboration, A. Abashian *et al.*, Nucl. Instrum. Meth. A **479**, 117 (2002).
[7] Y. Ushiroda, Nucl. Instrum. Meth. A **511**, 6 (2003).
[8] Belle Collaboration, S.H. Lee *et al.*, Phys. Rev. Lett. **91**, 261801 (2003).
[9] R. A. Fisher, Ann. Eugen. **7**, 179 (1936).
[10] G. C. Fox and S. Wolfram, Phys. Rev. Lett. **41**, 1581 (1978).
[11] H. Kakuno *et al.*, hep-ex/0403022.
[12] J. E. Gaiser *et al.*, Phys. Rev. D **34**, 711 (1986).
[13] ARGUS Collaboration, H. Albrecht *et al.*, Phys. Lett. B **241**, 278 (1990).
[14] A. Ali and V. M. Braun and H. Simma, Z. Phys. C **6**, 437 (1994).
[15] A. Ali, E. Lunghi, A. Parkhomenko, Phys. Lett. B **595**, 323 (2004).
[16] Particle Data Group, S. Eidelman *et al.*, Phys. Lett. B **592**, 1 (2004).

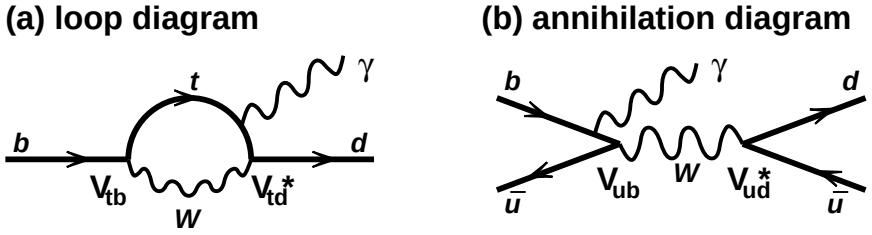

FIG. 1: (a) Loop diagram for $b \to d\gamma$ and (b) annihilation diagram only for $B^- \to \rho^-\gamma$.

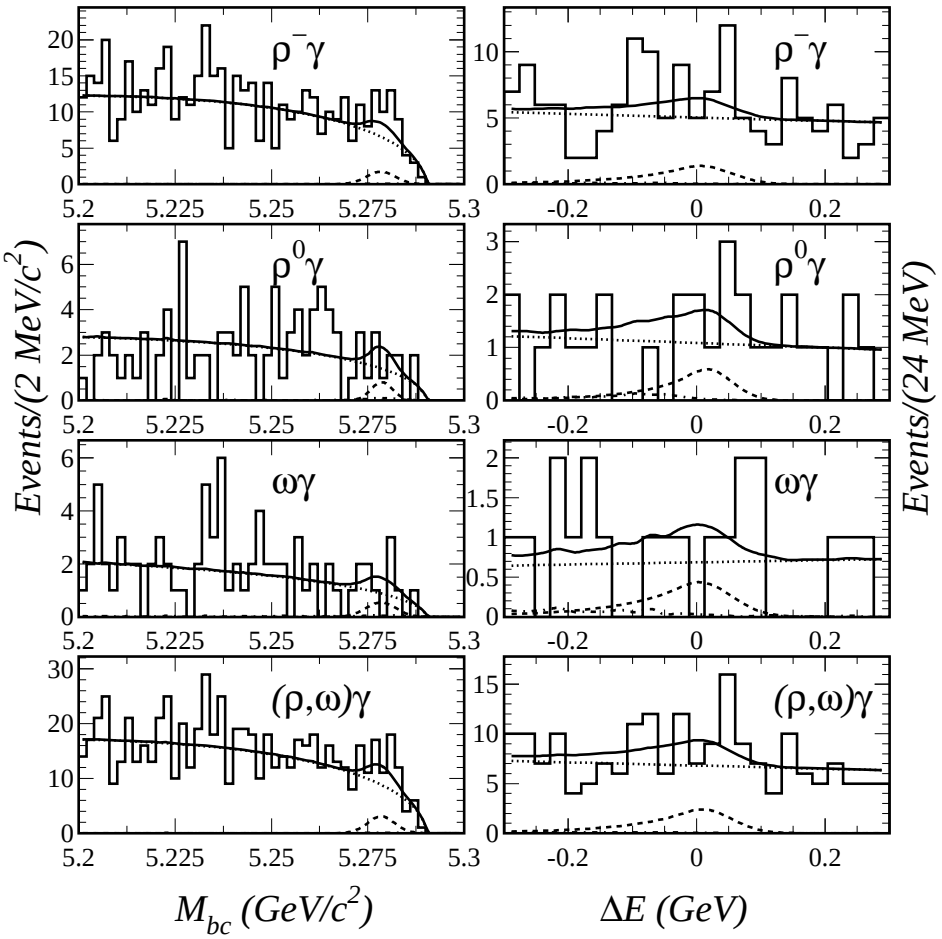

FIG. 2: Projections of the simultaneous fit results to $M_{\rm bc}$ (in the region -0.10 GeV $< \Delta E <$ 0.08 GeV) and ΔE (in the region 5.273 GeV/$c^2 < M_{\rm bc} <$ 5.285 GeV/c^2) for the individual modes and the sum of them. Lines represent the total fit result (solid), signal (dashed), continuum (dotted), and B decay background (dot-dashed) components.

TABLE I: Efficiencies, significances, and 90% confidence level upper limits for the branching fractions.

Mode	Efficiency (±syst)	Significance	Upper limit (90% C.L.)
$B \to (\rho,\omega)\gamma$ combined	—	1.9	1.4×10^{-6}
$B^- \to \rho^-\gamma$	$(5.5 \pm 0.4)\%$	2.1	2.2×10^{-6}
$\overline{B}^0 \to \rho^0\gamma$	$(3.9 \pm 0.3)\%$	0.6	0.8×10^{-6}
$\overline{B}^0 \to \omega\gamma$	$(3.9 \pm 0.4)\%$	0.2	0.8×10^{-6}